Jpn J Radiol (2016) 34:267–276
DOI 10.1007/s11604-016-0517-7

PICTORIAL ESSAY

18F-Fluorodeoxyglucose PET/CT in Langerhans cell histiocytosis: spectrum of manifestations

Krishan Kant Agarwal[1] · Rachna Seth[2] · Abhishek Behra[1] · Manisha Jana[3] · Rakesh Kumar[1]

Received: 13 November 2015 / Accepted: 28 December 2015 / Published online: 13 January 2016

Abstract The objective of this article is to provide an illustrative tutorial highlighting the utility of 18F-FDG PET/CT imaging to detect the spectrum of manifestations in patients with Langerhans cell histiocytosis. FDG PET/CT is a powerful tool for making an early diagnosis; it allows higher diagnostic confidence with regard to lesions, measuring the extent of disease (staging) and assessing disease activity, and is consequently useful for evaluating the response to therapy in patients with Langerhans cell histiocytosis.

Keywords FDG PET/CT · Langerhans cell histiocytosis · PET/CT

The objective of this article is to provide an illustrative tutorial highlighting the utility of 18F-FDG PET/CT imaging to detect the spectrum of manifestations in patients with Langerhans cell histiocytosis (LCH). FDG PET/CT is a powerful tool for making an early diagnosis; it allows higher diagnostic confidence with regard to lesions, measuring the extent of disease (staging) and assessing disease activity, and is consequently useful for evaluating the response to therapy in patients with Langerhans cell histiocytosis.

✉ Rakesh Kumar
rkphulia@yahoo.com

[1] Diagnostic Nuclear Medicine Division, Department of Nuclear Medicine, All India Institute of Medical Sciences, New Delhi 110029, India

[2] Department of Paediatrics, All India Institute of Medical Sciences, New Delhi, India

[3] Department of Radiology, All India Institute of Medical Sciences, New Delhi, India

Langerhans cells are antigen-presenting cells found in the skin, mucosa and lymph nodes. LCH is a rare disease arising from abnormal clonal proliferation and accumulation of pathological Langerhans cells [1]. LCH falls in the spectrum of histiocytosis, which is a group of disorders having the common feature of an increased number of tissue macrophages. In LCH, the Langerhans cells seem to be in a state of constant activation and additionally are prevented from leaving their peripheral tissues. The histiocytes accumulate and express inflammatory cytokines, leading to further recruitment of histiocytes and other inflammatory cells. This accumulation leads to the pathological sequel.

18F-FDG PET/CT has been studied for early diagnosis, measuring the extent of disease (staging) and consequently evaluating the response to therapy [2, 3]. The majority of Langerhans cell histiocytosis lesions have been found to be FDG avid; however, some FDG non-avid lesions have also been reported [3]. Additionally, a possible role for FDG PET/CT in the early diagnosis of neurodegenerative LCH has also been proposed [4].

The involvement of organ systems is classified as follows:

1. Unifocal: a single disease focus.
2. Multifocal:
   (a) Unisystemic: Multiple foci of disease, but only a single system involved.
   (b) Multisystemic: Multiple foci involving multiple organ systems.

Risk organs include the liver, spleen, bone marrow and lung. It must be specified that risk organ involvement may or may not be associated with organ dysfunction.

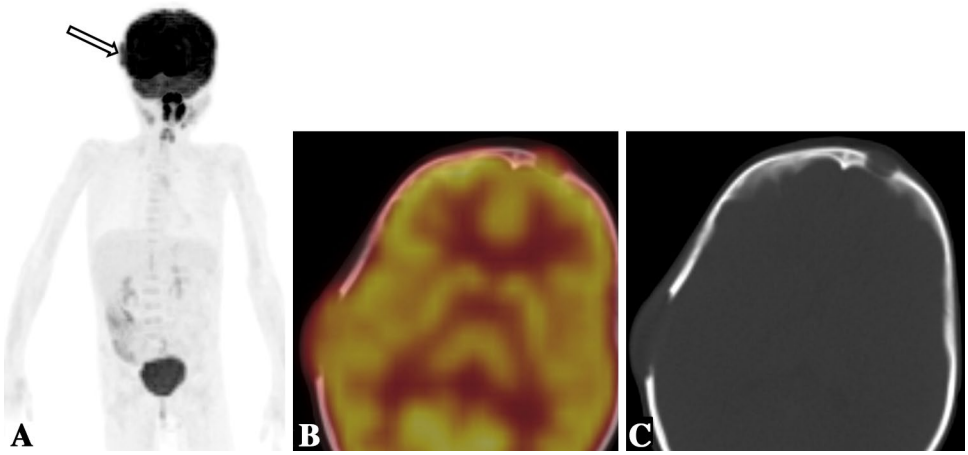

Fig. 1 A 5-year-old male child presenting with LCH. **a** Maximum-intensity-projection 18F-FDG PET image shows increased tracer uptake in the right temporoparietal region. **b and c** Axial FDG PET/CT and CT images show lytic lesions with a soft tissue component in the right temporal-parietal bone and left frontal bone (SUVmax 5.5)

Skeletal involvement

The most common sites of involvement in LCH are skeletal [5]. The lesions have osteoclast-like multinucleated giant cells that cause necrosis of the bone and consequently lead to formation of osteolytic lesions with soft tissue masses [6]. The lesions may be asymptomatic or present with local pain, tenderness and swelling around the lesion [5].

The most common sites of involvement are the skull and flat bones. Involvement of other bones, such as the femur, humerus, spine, ribs and mandible, is also seen. Involvement of the bones of the distal upper and lower extremities is extremely uncommon [5, 7]. In the skull, solitary or multiple punched out lesions and geographic lytic lesions with beveled margins and without a sclerotic rim may be seen. Greater involvement of the inner table compared to the outer table of the skull is noted (hole within a hole appearance; beveled edge). Occasionally, a button sequestrum may be noted in the center of the lytic bone lesion. Healed lesions may show sclerosis of the margins. Active disease lesions usually show FDG uptake; however, healed lesions may appear non-FDG avid (Fig. 1). Involvement of the pituitary stalk may lead to diabetes insipidus.

In the spine, the disease appears as osteolytic lesions with FDG uptake in active disease. Large lesions may lead to the collapse of the vertebral bodies (vertebra plana) with maintained intervertebral disc spaces (Fig. 2) [7]. Involvement of the mandible and facial bones presents as small lytic lesions (Figs. 3, 4 and 5). Involvement of the lamina dura may lead to loosening of teeth (floating tooth) [8]. In the mandible, more commonly the involvement of the superficial alveolar bone is noted. Involvement of the long bones has different imaging features depending on the disease phase imaged. The lesions noted in the extremities usually involve the diaphysis or metadiaphysis, respecting the growth plates. Endosteal scalloping, a continuous linear periosteal reaction, cortical thinning, intracortical tunneling and an associated soft tissue mass may be demonstrated [7]. FDG avidity of the lesion is present in active disease.

Marrow infiltration in LCH can occur and may lead to pancytopenia. However, it is not the only cause of pancytopenia in LCH [5]. Care needs to be taken in reporting bone marrow involvement in LCH, especially in post-chemotherapy patients with reactive marrow proliferation and also in patients receiving exogenous growth factors [9]. Certain features, such as focal FDG uptake, extension of bone metastasis, etc., lend higher predictive value to the diagnosis of marrow infiltration (Fig. 4).

Skin involvement

Skin involvement reportedly occurs in 50 % of cases of LCH. Isolated Langerhans cell histiocytosis of the skin occurs in about 10 % of patients. In general, skin-only histiocytosis has a good prognosis [5]. Reportedly 50 % of cases of skin-only LCH will progress to systemic disease. On FDG PET/CT, areas of active skin disease may be visible as mild increased uptake in the region of the involved skin. It may be appreciably better in the maximum intensity projection images as areas of increased uptake. Traditionally, however, uptake in skin disease is considered a weakness of FDG PET/CT. Skin lesions in LCH show a wide variety of presentations, ranging from nodular to papular

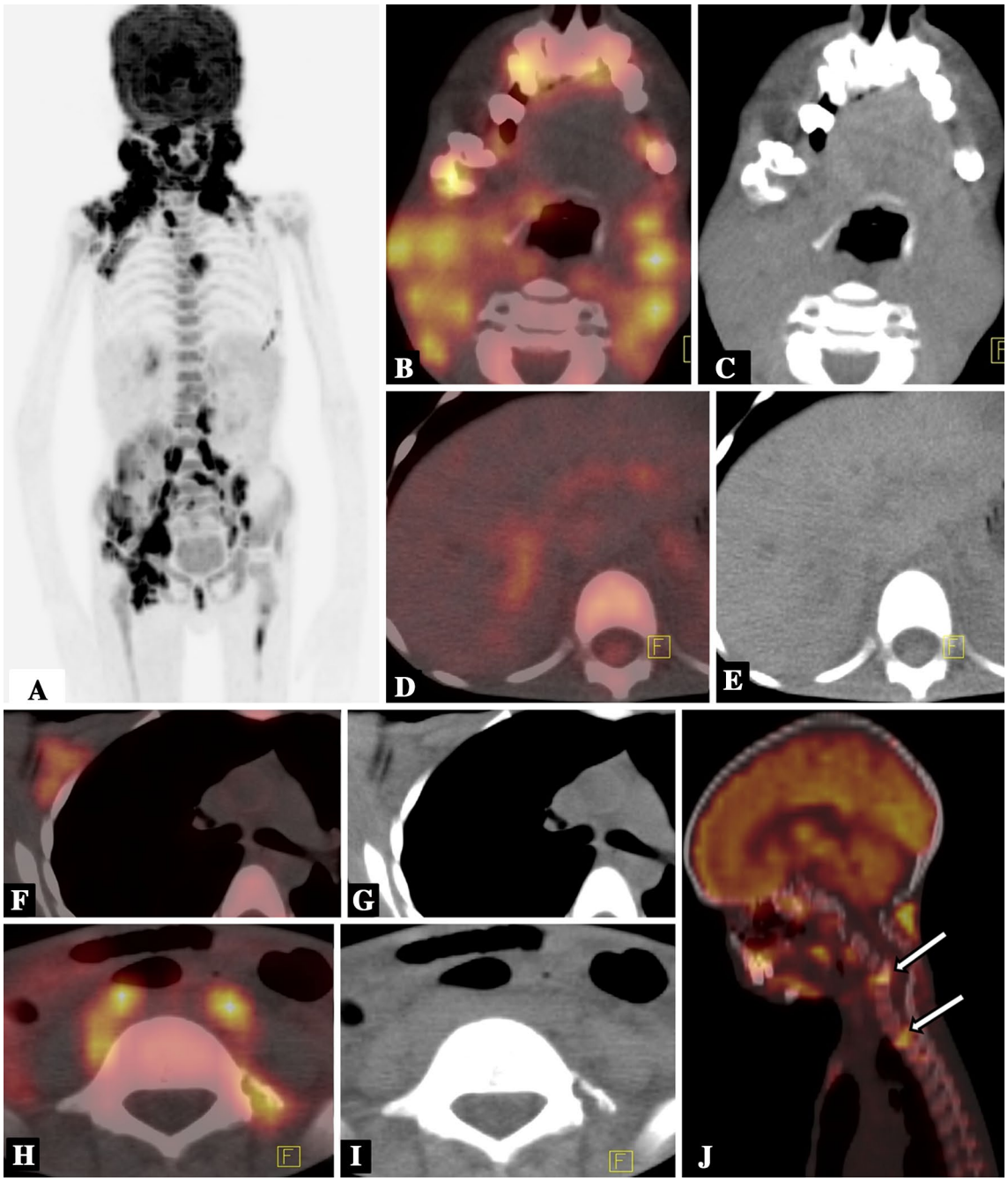

Fig. 2 An 11-year-old male child presenting with LCH. He was referred for an 18F-FDG PET/CT scan to determine the extent of disease involvement. **a** Maximum-intensity-projection 18F-FDG PET image shows multiple areas of increased tracer uptake involving bilateral cervical, supraclavicular, right axillary and abdominopelvic lymph node, liver and multiple skeletal sites. **b and c** Axial FDG PET/CT and CT images show multiple bilateral cervical lymph nodes with increased tracer uptake (SUVmax 9.7). **d and e** Axial FDG PET/CT and CT images show dilated biliary radicles with increased FDG uptake (SUVmax 5.3). **f and g** Axial FDG PET/CT and CT images show right axillary lymph nodes with increased tracer uptake. **h and i** Axial FDG PET/CT and CT images show retroperitoneal lymph nodes with increased tracer uptake. **j** Sagittal FDG PET/CT image shows increased tracer uptake involving the skull bone, sternum and cervical vertebrae (arrow)

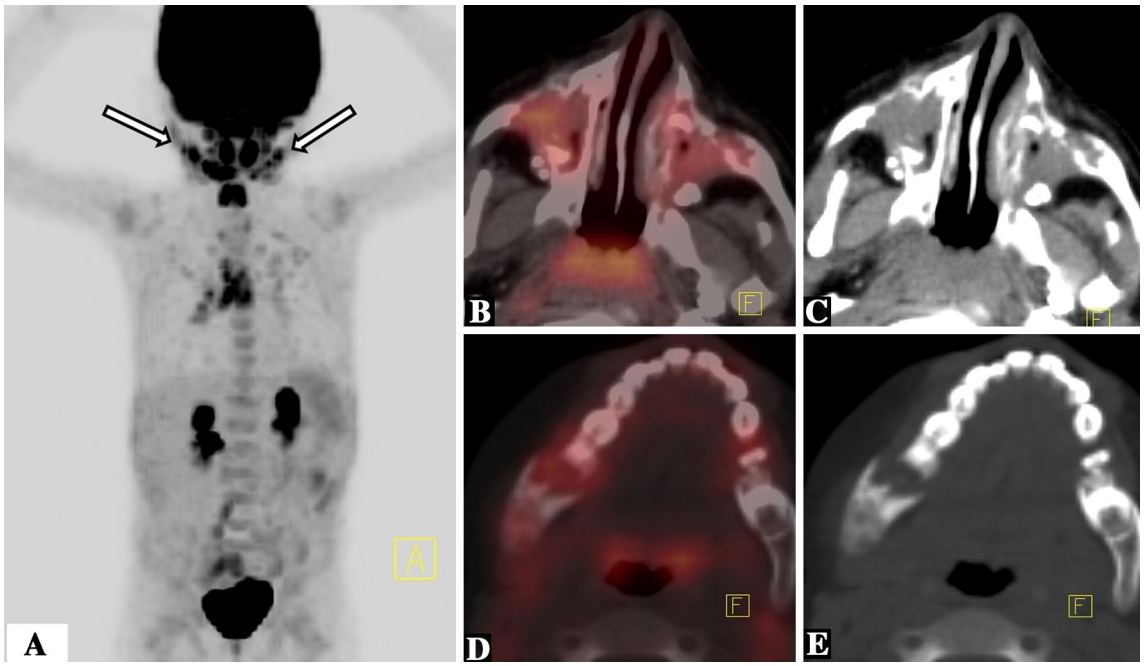

Fig. 3 A 4-year-old male child presenting with LCH. **a** Maximum-intensity-projection 18F-FDG PET image shows increased tracer uptake involving bilateral maxillary (*arrows*) and right mandibular regions. **b and c** Axial FDG PET/CT and CT images show bilateral maxillary sinuses with bone destruction and opacification with increased FDG uptake (SUVmax 5.9). **d and e** Axial FDG PET/CT and CT images show a lytic lesion in the right ramus and body of the mandible with increased FDG uptake (SUVmax 5.7)

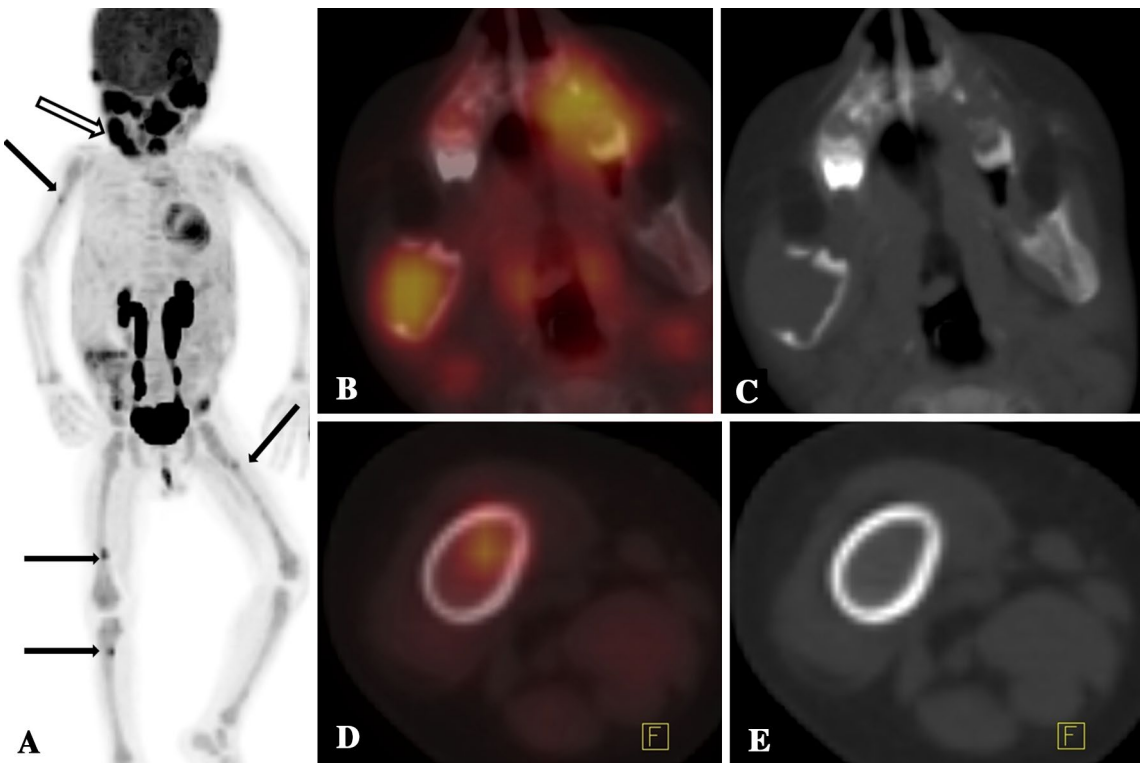

Fig. 4 A 1-year-old male child presenting with LCH. **a** Maximum-intensity-projection 18F-FDG PET image shows multiple focal areas of increased tracer uptake involving the skull, left maxillary region, right mandibular region (*arrow*) and right humerus, both the femoral and right tibial shaft regions (*black arrows*). **b and c** Axial FDG PET/CT and CT images show lytic lesions with increased tracer uptake in the right mandible and left maxillary bone (SUVmax 5.9). **d and e** Axial FDG PET/CT and CT images show focal increased FDG uptake in the shaft of right tibia with no corresponding CT changes (marrow lesion) (SUVmax 4.9)

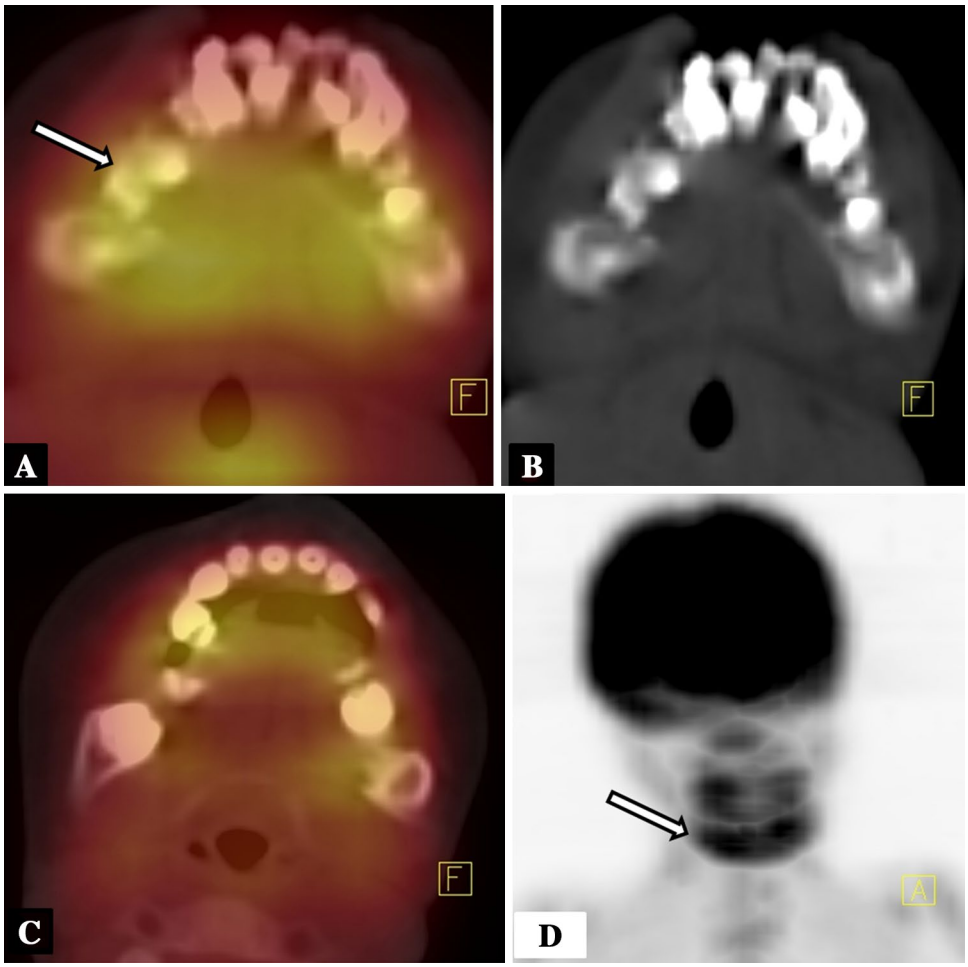

Fig. 5 A 4-year-old female child presenting with mandibular LCH. **a, b, and c** Axial FDG PET/CT and CT and PET images **d** show diffuse FDG uptake noted in the mandible (SUVmax 6.7)

lesions [10]. The extent of skin disease may vary in patients ranging from local disease to widely disseminated skin disease. This may occasionally affect the management of skin disease in LCH (Fig. 6).

Pulmonary involvement

Pulmonary involvement can either be as a part of the multisystemic disease process in childhood LCH or as a distinct process (pulmonary LCH) seen in young adult smokers and less often in children.

Pulmonary LCH on FDG PET/CT may have variable appearances depending on the disease stage. Bilateral and symmetrical, predominantly upper and middle lung zone nodules are seen. These nodular opacities may progress to multiple thin-/thick-walled cysts (often bizarre in shape), eventually leading to marked parenchymal fibrosis and a honeycomb pattern (Figs. 7, 8). CT findings of pulmonary LCH are similar in adult and pediatric populations with the exception that the lung base near the costophrenic angle is spared in adults but almost always involved in children [11]. Depending on the disease activity, FDG uptake is seen in the involved areas of the lung, whereas extensive disease may lead to diffuse FDG uptake in the lung.

Auricular involvement

Chronic otorrhea is a common presenting complaint in young patients with LCH because of the chronic otitis media and mastoiditis it causes. On FDG PET/CT, increased FDG uptake is seen in the region of the middle ear and, depending on the involvement, also as increased FDG uptake in the mastoid and any other involved part of the temporal bone [12] (Figs. 9, 10).

Orbital involvement

Orbital involvement usually occurs in the form of lytic lesions in the bony orbit with an associated soft tissue mass clinically present as local orbital infiltrates. LCH involvement of the eyelid, conjunctiva, caruncle, epibulbar

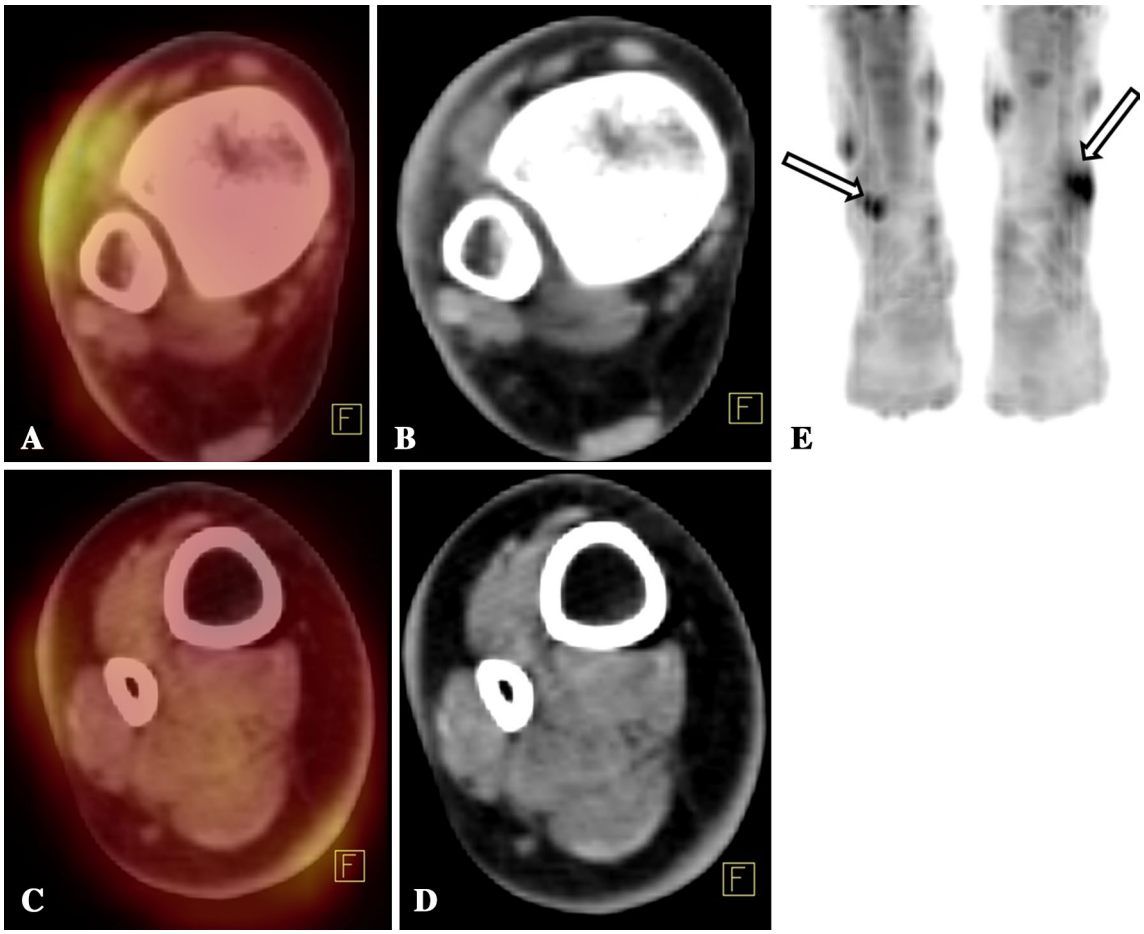

Fig. 6 A 14-year-old female child presenting with cutaneous LCH. **a, b, c, and d** Axial FDG PET/CT and CT and PET images **e** show multiple ill-defined cutaneous thickening with increased FDG uptake noted in bilateral lower limbs (SUVmax 6.4)

nodule, choroid, orbital apex and cavernous sinus have been described [13].

Liver involvement

Liver involvement in LCH may occur as part of multisystem disease or as the sole involvement. The pattern of disease seen on FDG PET/CT in the liver depends on the extent of disease involvement. Hepatomegaly with periportal lesions/nodules may be the only initial radiological findings (periportal halo). With disease progression, these nodules may enlarge and involve the entire liver parenchyma. The imaging characteristics of the lesion may also change with its phase (proliferative or xanthomatous phase), ranging from hypodense ring enhancement to hyperattenuating fibrotic lesions later [14]. Eventually these liver lesions may lead to a pattern of sclerosing cholangitis leading to biliary cirrhosis on CT. Active lesions show increased FDG uptake on PET. Cirrhotic changes and inflammatory cholangitis may lead to generalized increased FDG uptake in the liver (Figs. 2, 7).

Spleen involvement

Involvement of the spleen may be present in LCH [8]. The presentation may be as splenomegaly with generalized FDG uptake or as multiple nodular hypo-/hyperattenuating lesions on CT. FDG uptake of the lesions depends on the disease activity (Fig. 7).

Gastrointestinal involvement

Intestinal involvement in LCH is usually secondary to extensive multisystemic involvement. It is considered a bad prognostic marker for survival. Initially, disease

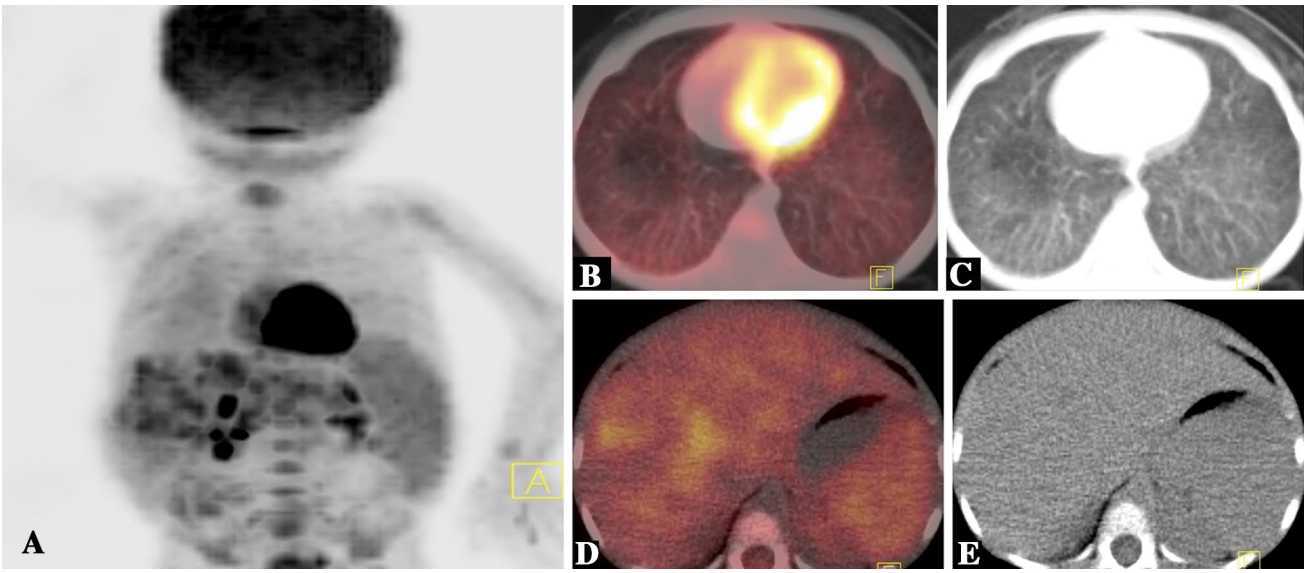

Fig. 7 A 1-year-old male child presenting with LCH. **a** Maximum-intensity-projection 18F-FDG PET image shows increased tracer uptake involving the liver, spleen and bilateral hemithorax regions. **b and c** Axial FDG PET/CT and CT images show ground-glass opacity in the bilateral lungs with diffusely increased FDG uptake. **d and e** Axial FDG PET/CT and CT images show multiple hypodense lesions in both liver lobes with heterogeneous FDG uptake (SUVmax 5.4) and also show an enlarged spleen with diffusely increased FDG uptake

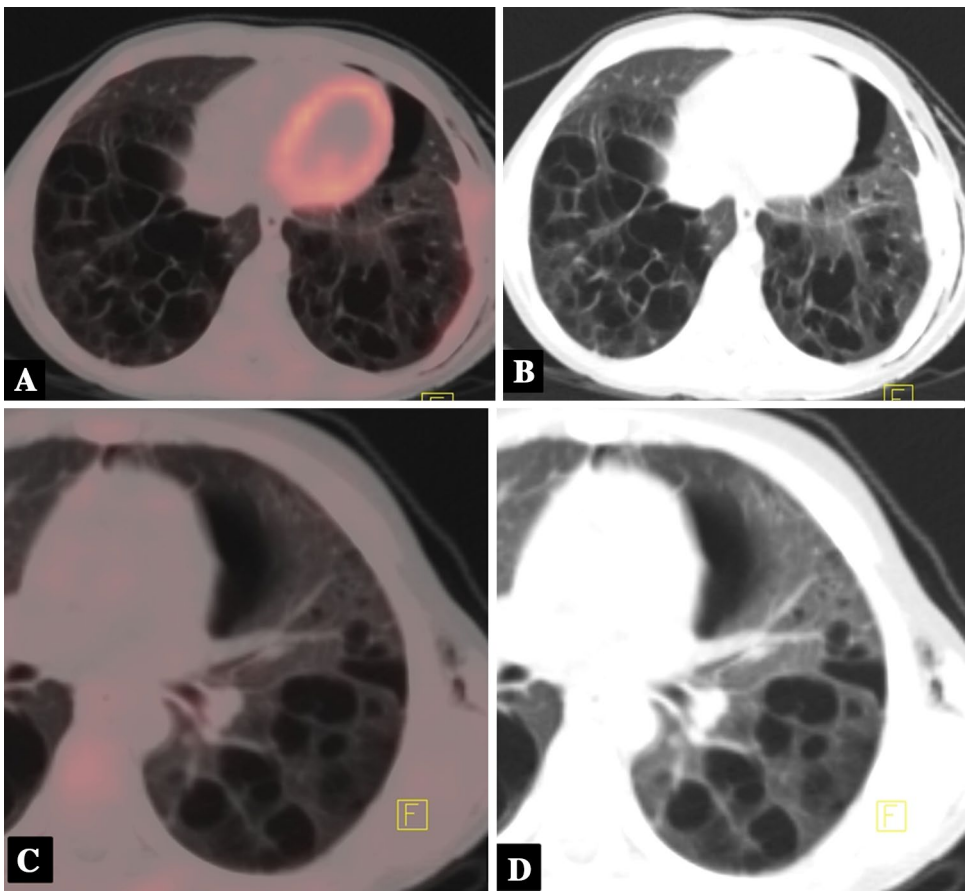

Fig. 8 A 10-year-old female child presenting with pulmonary LCH. **a, b, c, and d** Axial FDG PET/CT and CT images show multiple thin-walled irregular cystic spaces with reticular thickening and nodular changes noted involving the bilateral lungs

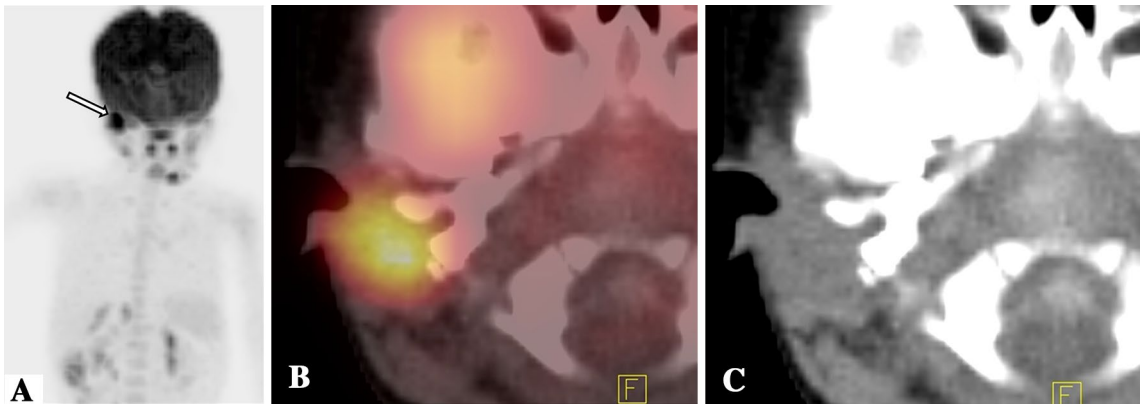

Fig. 9 A 1-year-old female child presenting with LCH. **a** Maximum-intensity-projection 18F-FDG PET image shows increased tracer uptake in the right auricular region. **b and c** Axial FDG PET/CT and CT images show a soft tissue density mass in the right external auditory canal presenting intensely increased FDG uptake, which is seen to extend into the mesotympanum and cause breakage in the lateral wall of the right mastoid antrum (SUVmax 9.4)

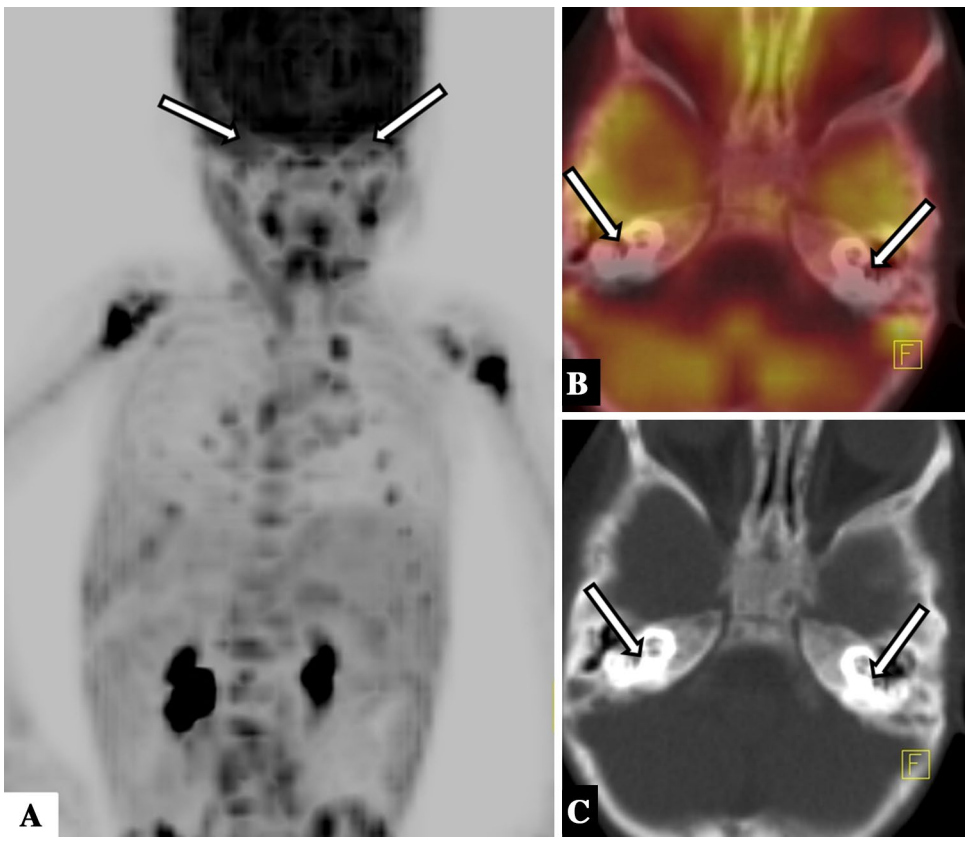

Fig. 10 A 2-year-old male child presenting with LCH. **a** Maximum-intensity-projection 18F-FDG PET image does not show abnormal tracer uptake in the bilateral temporal region (due to physiological FDG uptake in the brain). **b and c** Axial FDG PET/CT and CT images show loss of pneumatization of mastoid air cells with increased tracer uptake (SUVmax 5.4)

involvement occurs as small intramucosal nodules that progress to cause intestinal wall thickening. The most common site of involvement is the distal ileum. Colonic involvement is also a common form of intestinal involvement [8]. Determining intestinal involvement is a potential weakness of FDG PET/CT because of the risk of false positives from physiological intestinal uptake. Active disease shows increased FDG uptake.

CNS involvement

The majority of intracranial LCH lesions occur secondary to the extension of the disease from large skull-based lesions. Otherwise, lesions associated with LCH show a preponderance in areas without a blood brain-barrier such as the meninges, ependymal area, choroid plexus, pineal gland, etc. Similarly, hypothalamic involvement can occur

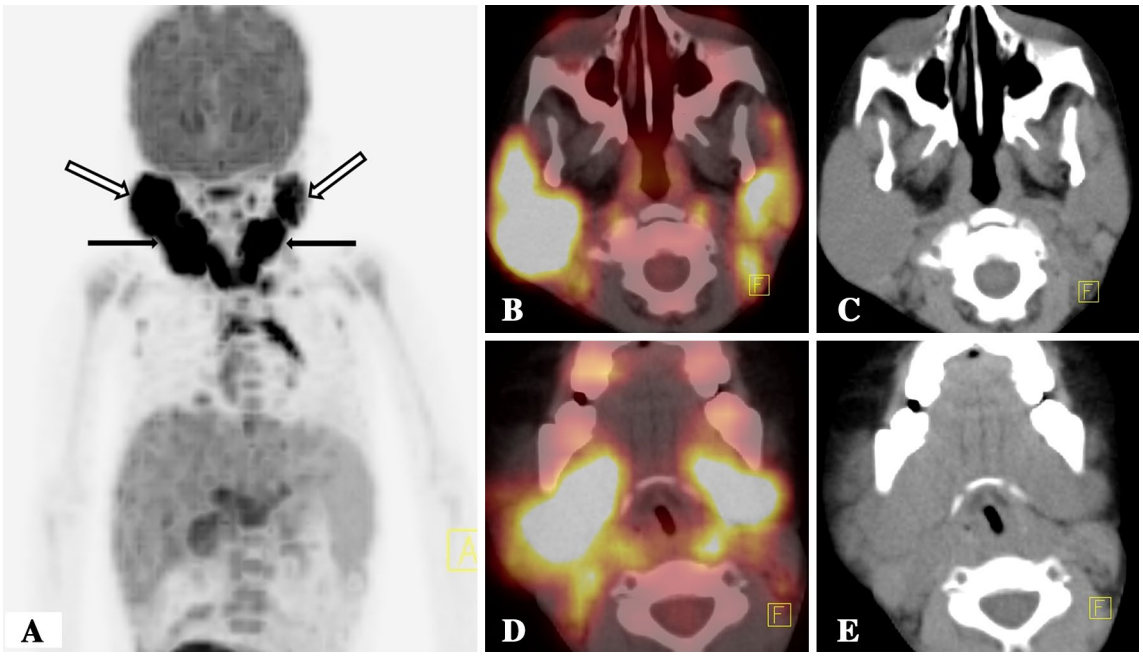

Fig. 11 A 4-year-old male child presenting with LCH. **a** Maximum-intensity-projection 18F-FDG PET image shows increased tracer uptake involving the bilateral parotid (*outlined white arrows*) and submandibular glands (*black arrows*), bilateral cervical, supraclavicular, axillary and mediastinal lymph nodes. **b and c** Axial FDG PET/CT and CT images show bilateral enlarged parotid glands showing intensely increased FDG uptake (SUVmax 10.7). **d and e** Axial FDG PET/CT and CT images show bilateral enlarged submandibular glands showing intensely increased FDG uptake (SUVmax 10.3)

as it has extensions beyond the blood-brain barrier and also forms a functional unit with circumventricular organs. This involvement leads to diabetes insipidus. Imaging findings of CNS involvement include pituitary infundibular thickening and enhancement on contrast-enhanced MRI and the absence of a posterior pituitary bright spot. Mass lesions seen at this site show increased FDG uptake. Deficits produced in the anterior pituitary are usually permanent [5].

Clinical sequelae on CNS may include a paraneoplastic neurodegenerative disorder. This occurs secondary to involvement of the cerebellum, basal ganglia and pons. Early diagnosis of neurodegenerative CNS LCH by measuring the pathological reduction of physiological FDG uptake in these regions of the brain using FDG PET has also been suggested.

Lymph nodes involvement

Lymph nodal involvement in LCH usually occurs as a part of multisystemic LCH; however, isolated lymph node involvement has also been reported. The most commonly involved sites reported in LCH are the cervical lymph nodes followed by the axillary, inguinal and supraclavicular lymph nodes [8]. Lymph node involvement appears as enlarged lymph nodes with increased FDG uptake (Figs. 2, 11).

Besides these sites of involvement, various other rare locations have also been described in LCH.

Thymic involvement may occur in children, with thymic enlargement, calcifications and cystic spaces seen on CT. On FDG PET/CT care must be taken to report thymic involvement on account of mild physiological uptake in the thymus. Additionally, in treated cases, diffuse thymic FDG uptake may increase as a reactive phenomenon [15].

Salivary gland involvement in LCH is extremely rare, but has been described. Imaging features show bilateral homogeneous enlargement of the salivary gland without any areas of necrosis or calcification. Cervical lymphadenopathy may be associated with salivary gland involvement [16] (Fig. 11).

Conclusion

LCH can present with a wide spectrum of involvement and prognosis. FDG PET/CT as an imaging tool has great utility in LCH. It allows for global assessment of the disease extent with high sensitivity for lesion detection. Additionally, it allows higher diagnostic confidence with regard to lesions and also assesses disease activity. This also helps in making management decisions in this group of patients. FDG uptake is associated with the activity of the disease

process. Most imaging findings shown as LCH are generally not specific (not pathognomonic), and the differential diagnosis should be considered in the interpretation of images. In the adult population the most common differential diagnosis of a lytic lesion with a soft tissue component is metastatic disease from thyroid, renal, lung and multiple myeloma malignancies. However, in the pediatric population occasionally lymphoma, primary bone tumors and tuberculosis are more common differential diagnoses.

Compliance with ethical standards

Conflict of interest statement None of the authors have any conflict of interest.

Financial disclosures None of the authors have any financial disclosures.

References

1. Chu T, Jaffe R. The normal Langerhans cell and the LCH cell. Br J Cancer Suppl. 1994;23:S4–10.
2. Freebody J, Wegner EA, Rossleigh MA. 2-deoxy-2-((18)F) fluoro-D-glucose positron emission tomography/computed tomography imaging in paediatric oncology. World J Radiol. 2014;6:741–55.
3. Phillips M, Allen C, Gerson P, McClain K. Comparison of FDG PET scans to conventional radiography and bone scans in management of Langerhans cell histiocytosis. Pediatr Blood Cancer. 2009;52:97–101.
4. Steiner M, Prayer D, Asenbaum S, Prosch H, Minkov M, Unger E, et al. Modern imaging methods for the assessment of Langerhans' cell histiocytosis-associated neurodegenerative syndrome: case report. J Child Neurol. 2005;20:253–7.
5. Weitzman S, Egeler RM. Langerhans cell histiocytosis: update for the pediatrician. Curr Opin Pediatr. 2008;20:23–9.
6. Da Costa CET, Annels NE, Faaij CMJM, Forsyth RG, Hogendoorn PCW, Egeler RM. Presence of osteoclast-like multinucleated giant cells in the bone and nonostotic lesions of Langerhans cell histiocytosis. J Exp Med. 2005;201:687–93.
7. Khung S, Budzik J-F, Amzallag-Bellenger E, Lambilliote A, Soto Ares G, Cotten A, et al. Skeletal involvement in Langerhans cell histiocytosis. Insights Imaging. 2013;4:569–79.
8. Schmidt S, Eich G, Geoffray A, Hanquinet S, Waibel P, Wolf R, et al. Extraosseous Langerhans cell histiocytosis in children. Radiogr Rev Publ Radiol Soc N Am Inc. 2008;28:707–26 **(quiz 910–1)**.
9. Kazama T, Swanston N, Podoloff DA, Macapinlac HA. Effect of colony-stimulating factor and conventional- or high-dose chemotherapy on FDG uptake in bone marrow. Eur J Nucl Med Mol Imaging. 2005;32:1406–11.
10. Querings K, Starz H, Balda B-R. Clinical spectrum of cutaneous Langerhans' cell histiocytosis mimicking various diseases. Acta Derm Venereol. 2006;86:39–43.
11. Juvet SC, Hwang D, Downey GP. Rare lung diseases III: pulmonary Langerhans' cell histiocytosis. Can Respir J J Can Thorac Soc. 2010;17:e55–62.
12. Mueller RJ, Siegel A, Seltzer M, McKnight TA. Langerhans cell histiocytosis of the auditory canal detected by 18F-FDG PET/CT. Clin Nucl Med. 2012;37:908–9.
13. Herwig MC, Wojno T, Zhang Q, Grossniklaus HE. Langerhans cell histiocytosis of the orbit: five clinicopathologic cases and review of the literature. Surv Ophthalmol. 2013;58:330–40.
14. Yi X, Han T, Zai H, Long X, Wang X, Li W. Liver involvement of Langerhans' cell histiocytosis in children. Int J Clin Exp Med. 2015;8:7098–106.
15. Turpin S, Carret A-S, Dubois J, Buteau C, Patey N. Isolated thymic Langerhans cell histiocytosis discovered on F-18 fluorodeoxyglucose positron emission tomography/computed tomography (F-18 FDG PET/CT). Pediatr Radiol. 2015;45:1870–3.
16. Iqbal Y, Al-Shaalan M, Al-Alola S, Afzal M, Al-Shehri S. Langerhans cell histiocytosis presenting as a painless bilateral swelling of the parotid glands. J Pediatr Hematol Oncol. 2004;26:276–8.